© A Publication of the Centre for Research and Development (CERAD), The Federal University of Technology, Akure, Nigeria (www.jost.futa.edu.ng)

JOST 2021

GIS-based Analysis of Drainage Morphometry and Landuse/Landcover Dynamics in the River Ogun-Osun Basin, Southwestern Nigeria

Okogbue, E.C.[1]; Balogun, I.A. [1,3]; Akinbobola, A.[1]; Adeyeri, O.[1,4]; Oluleye, A.[1]; Ajayi, V.O.[1]; Akinluyi, F.O.[2]; Akinwumiju, A.S.[2] and Ige, S.O.[5]

[1]*Department of Meteorology & Climate Science, Federal University of Technology, Akure, Nigeria*

[2]*Department of Remote Sensing & GIS, Federal University of Technology, Akure, Nigeria*

[3]*Doctoral Research Programme in West African Science, West African School on Climate and Adapted Land Use, Akure, Nigeria*

[4]*Institute for Meteorology and Climate Research Atmospheric Environmental Research, Karlsruhe Institute of Technology, Campus Alpine, Germany*

[5]*Nigerian Meteorological Agency, Lagos, Nigeria*

Corresponding Author: Balogun, I.A.: iabalogun@futa.edu.ng

ABSTRACT: Morphometry is a technique for locating groundwater resources by analyzing landforms and drainage systems. The drainage pattern is crucial for determining the basin's hydrology using morphometric data. In addition, the morphometric parameters of the basin determine the type of streaming system used to get water to the streams. The River Ogun-Osun Basin (ROSB) covers an area of 22800 km^2, and according to Strahler's classification method of the digital elevation model (DEM), the drainage network retrieved from the basin shows a dendritic drainage pattern. Therefore, the research region is classified as a fourth-order basin, with lower order streams dominating the basin. In association with the land use land cover characteristics, the land use transformation could modify the morphometric properties of the basin. For example, the relative change shows that rock outcrop and forest decreased by 135.9% and 97.7%, respectively, from 2000 to 2019 using the Landsat ETM+ and OLI datasets. The dynamics of this change shows that most rock outcrops have been converted to bare soil due to quarry activities. Similarly, most forests have been converted to croplands. This is capable of modifying the streamflow and the overall discharge in the basin. Decision-makers can use the findings of this study to plan and manage the basin more sustainably.

Keywords: DEM, GIS, Basin, Morphometric analysis, Landuse/landcover

JoST. 2021. 11(2): 145-164

Accepted for Publication: November 29, 2021

INTRODUCTION

A basin is a geo-hydrological unit that drains runoff water to a single place and can be identified by looking at ridge and gully regions. A basin can be described hydrologically as an area from which runoff drains to a specific location in a drainage system. Basins are suitable hydrologic units for conducting development activities linked to water management because water follows a predictable flow path (Patel *et al.* 2013; Singh *et al.* 2018).

In the delineation, updating, and morphometric analysis of drainage basins, remote sensing and GIS approaches have proven effective (Ezeh and Mozie 2019; Pardeshi 2018; Hajam *et al.* 2013). Any hydrological inquiry, such as assessing water potential, availability and water management, requires drainage basin analysis. Physiographic properties of drainage basins, such as size, shape, the slope of drainage area, drainage density, number and length of rivers, landuse/landcover (LULC), can be linked to a variety of crucial hydrologic phenomena (Rastogi and Sharma 1976). Traditional approaches have been used to investigate the morphometric properties of various river basins

and sub-basins worldwide (e.g., Patel *et al.* 2013; Hajam *et al.* 2013; Adeyeri *et al.* 2017a; Taofik *et al.* 2017; Odiji *et al.* 2021). However, with the introduction of remotely sensed data, it is now possible to better understand resources from broader basinal areas in a much shorter time and with more detail than traditional ground surveys.

In Nigeria, topographic maps have been employed to examine the morphometric properties of the Ogunpa and Ogbere Drainage Basins, Ibadan (Ajibade et al., 2010). Bunmi et al. (2017) investigated the morphometry of the Asa and Oyun River Basins in North Central Nigeria using Digital Elevation Model (DEM). Geospatial approaches were used by Ezeh and Mozie (2019) to conduct a morphometric investigation of the Idemili Basin.

The ROSB is one of Nigeria's most significant hydrological basins. There is, however, a scarcity of precise knowledge on the basin's morphometric properties and LULC dynamics. For example, changes in river discharges, an important hydrological variable of a basin have been caused by human activities such as land-use land-cover (LULC) change, dam construction and operation, groundwater and surface water, irrigation canals, and mining (Destouni et al. 2013; Adeyeri et al. 2020). Studies in China's Heihe River basin (Qiu et al. 2016) and Africa's Lake Chad basin (Buma et al. 2016) confirmed that human activities affect basin discharge.

The size and location of the basin, elevation, land management, and LULC types all influence the link between LULC variations and river discharge (Li et al. 2001).

Over the Naoli Basin in China, for example, Hao et al. (2004) found that discharge rises as forest cover increases. On the other hand, Jia et al. (2009) found that increase in forest cover decreases the river discharge. Legesse et al. (2003) also found that switching from plantation to forest reduced outflow in the Ketar Basin, North Africa.

The impact of rainfall variability and LULC variations on the water balance components of the White Volta Basin, West Africa, was explored by Awotwi et al. (2017). The researchers discovered that converting grassland and savannah to plantation lowered the quantity of available blue water (water in freshwater lakes, rivers, and aquifers) while increasing the amount of available green water (water needed by plants derived from soil moisture after rainfall). Mohamad and Markus (2009) also claimed that dense urbanization raises discharge peaks. In Nigeria, Adeyeri et al. (2020) assessed the impact of human activities and rainfall variability on the river discharge of Komadugu-Yobe Basin. They concluded that the increment in discharge was caused by approximately 50% rainfall variability and 50% human activities due to alteration to the LULC.

In terms of land degradation and food security, any country's economic and ecological health are inextricably related to the state of the basin. A poorly managed basin usually causes hydrological changes and environmental deterioration (Forest Management Bureau 2011). As a result, understanding the ROSB's characteristics, components, behaviour, and natural resource management for long-term growth is crucial. The purpose of this research is to assess the morphometric parameters of the ROSB, and understand the LULC dynamics. The study will help improve the management, land use planning, water conservation, and resource management of the basin.

MATERIALS AND METHODS

Study Area

The ROSB lies within 6° N and 9° N latitudes and 2°35′E and 4°55′E longitudes. The basin covers a total of 22800 km^2. This basin is bordered to the east by the Republic of Benin (Figure 1). The basin is between 0 and 550 meters above sea level. Primarily, the basin is drained by two main rivers, Ogun and Osun, with a number of tributaries and smaller rivers namely: Sasa, Ona, Ibu, Ofiki and Yewa. Many rivers in sub-Saharan Africa have low flow especially in dry season, a situation that gives rise to serious concern for long-term domestic, animal and irrigation supplies in the region (Rangeley et al., 1994).

The ROSB is defined by a tropical savannah climate in the north and a tropical rain forest climate in the south, according to the Koppen climatic classification. The climatological minimum and maximum air temperatures range from 21 to 26 degrees Celsius and 26 to 35 degrees Celsius, respectively.

The mean annual rainfall ranges between 1,150mm in the north to around 2,285 mm in the southern extremity. Two seasons are distinguishable in the River Basin; a dry season from November to March and a wet season between April and October. The total annual potential evapotranspiration is estimated at between 1600 and 1900 mm (Bolaji and Bhattacharya, 2010).

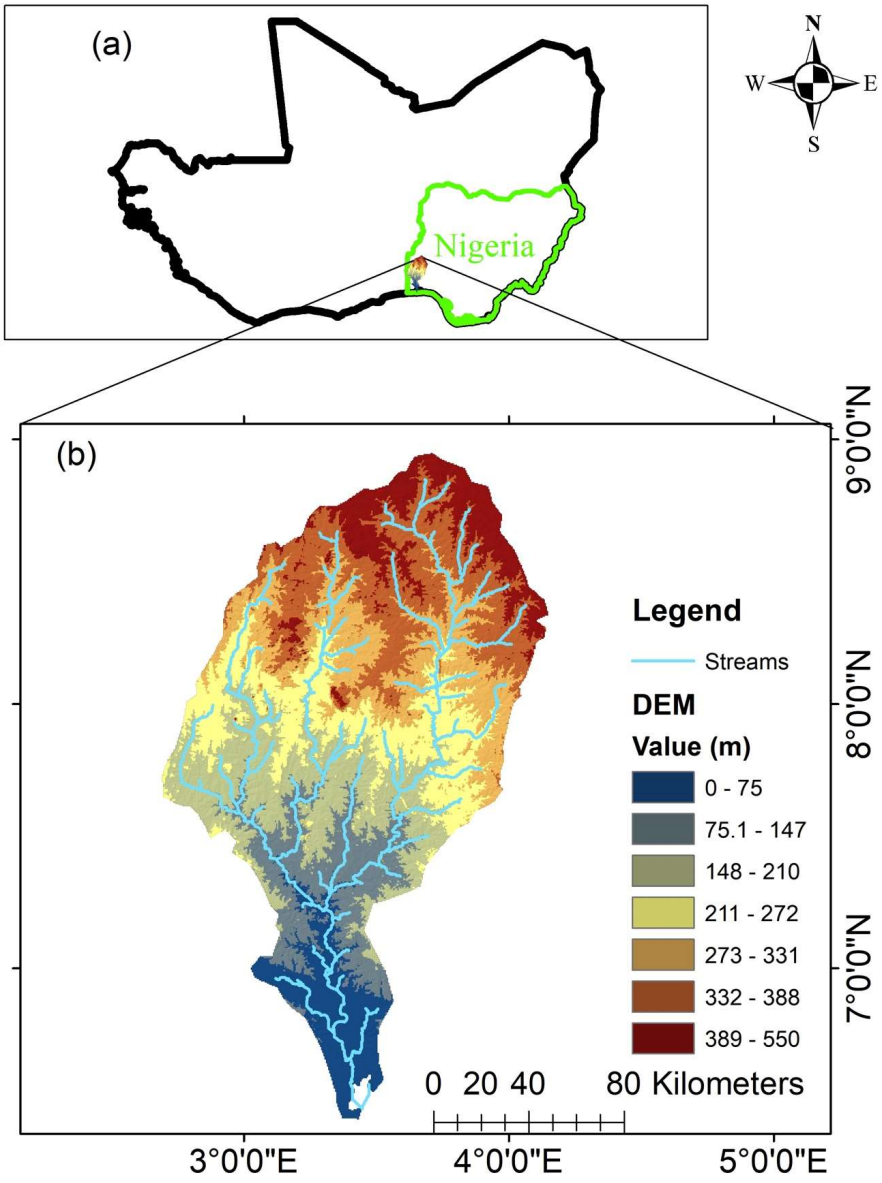

Figure 1: Map of the study area

Source of Data

The Digital Elevation Model (DEM) of the Shuttle Radar Topographic Mission (SRTM) with a resolution of 30 meters was obtained from https://earthexplorer.usgs.gov/ was used to extract stream networks, slopes, and terrain characteristics, whereas LULC dynamics were studied using 30m resolution Landsat ETM+ and OLI images with path 191 row 55 and path 191 row 56.

Stream Network

The basin's stream network was produced from the DEM. To reduce uncertainties associated with the sinks in DEM, the DEM was filled (Mayomi et al. 2019; Das and Pardeshi 2018; Hajam et al. 2013). Using Strahler's method of stream ordering (Strahler 1957; Mayomi et al. 2019; Adeyeri et al. 2017a), the streams network and subsequent ordering were derived from the flow accumulation and direction generated from the DEM.

The derivation of the stream network was based on a threshold accumulation value of 800, which means that each drainage network cell must have at least 800 contributing cells, resulting in a less dense stream network than a lower threshold value depending on the size of the basin (Arabameri et al. 2020).

Delineation of the Basin

The Soil and Water Assessment Tool (SWAT) delineation module (Luo et al. 2011) was used to delineate the basin and subsequently define the sub-basins. The DEM was imported into SWAT, then overlaid with stream network data to identify the sub-basins through the pour points. This method works by superimposing the DEM over the stream data to highlight the stream network's location and improve the DEM quality by filling the sink (necessary for hydrological studies), determining the flow accumulation and direction.

Topographic Wetness Index (TWI)

The Topographic Wetness Index (Beven and Kirkby 1979) is used to assess the potential for flow intensity and accumulation. It describes the impact of topography on the location and extent of saturated runoff source locations (Wilson and Gallant 2000). The higher the number, the wetter it is, and the lower the number, the dryer it is. The following formula is used to compute TWI:

$TWI = In\frac{\alpha}{\tan\beta+}$

Where α is the catchment area and is the slope, C is a constant

Vector Ruggedness Measure (VRM)

This calculates the vector ruggedness measure to determine the roughness of the terrain (Sappington et al. 2007).

Terrain Ruggedness Index (TRI)

This follows the implementation of the Riley et al. (1999) TRI.

TRI ranges as follows:

0-80 - level terrain surface.
81-116 - nearly level surface.
117-161 - slightly rugged surface.
162-239 - intermediately rugged surface.
240-497 - moderately rugged surface.
498-958 - highly rugged surface.
gt 959 - extremely rugged surface.

Solar-radiation Aspect Index (TRASP)

This calculates the Roberts and Cooper (1989) Solar-radiation Aspect Index. The circular aspect is rotated to assign a value of zero to land oriented in a north-northeast direction (typically the coolest and wettest orientation) and a value of one on the hotter, dryer south-southwesterly slopes. The result is a continuous variable between 0 - 1. The metric is defined as: $1 - \cos\left[\frac{\pi}{180}\right][a - 30] * 0.5$

where; a is the aspect in degrees.

Furthermore, other morphometric analyses like Steam length (Strahler 1957), Mean stream length (Strahler 1957), Drainage density (Horton 1945), Stream frequency (Horton 1945), Infiltration number (Faniran 1968), Length of overland flow (Horton 1945), Bifurcation ratio (Strahler 1964 a,b) and slope were considered.

LULC Classification and Transition Matrix

Landsat-8 Operational Land Imager (OLI) was acquired from the United State Geological Survey (USGS) website. Landsat-8 OLI

spectral bands 2 to 7 and band 9 were stacked and pre-processed for haze reduction, orthorectification and re-projected to Geographic Coordinate System (GCS), Minna datum. The stacked pre-processed imagery was subjected to optimum index factor analysis and spectral bands 563 (OIF = 44.46) were selected as the best 3-band to create colour composite. Prior to image classification, enhanced imagery (spectral bands: 563) was produced by histogram equalization that aided the identification of landscape features during the taking of training classes. Maximum likelihood classification algorithm was used to classify the Ogun River basin, the study area into: forest, settlement, water bodies, cropland, woodland savanna, bare soil and rock outcrop. The accuracy assessment was conducted by using Kappa coefficient and it equals 0.91. The spatio-temporal changes in the dynamics of the LULC are assessed using the LULC transition matrix and the rate of relative change among LULC classes.

The LULC transition matrix is a square matrix which aims at describing the probabilities of moving from one LULC state 'i' to another LULC state 'j' in a dynamic system. Each row presents the probabilities of transitioning from the initial state represented by that row to the other later state. The transition matrix P is given by using $P_{1,j}$ as the ith row and jth column element. This is presented as (Adeyeri et al. 2020);

$$P = \begin{bmatrix} P_{1,1} & P_{1,2} \dots & P_{1,j} \dots P_{1,S} \\ P_{i,1} & P_{i,2} \dots & P_{i,j} \dots P_{1,S} \\ \vdots & \vdots & \vdots \\ P_{S,1} & P_{S,2} \dots & P_{S,j} \dots P_{S,S} \end{bmatrix} \quad (1)$$

The rate of relative change in LULC classes (T) in percentage is given as;

$$T = \frac{L_{final} - L_{initial} * 100}{L_{initial}} \quad (2)$$

Where L_{final} and $L_{initial}$ represents the final and initial states of the LULC classes respectively over a particular period of time.

RESULTS AND DISCUSSION

Catchment Delineation

This sets a boundary around a control point or outlet that symbolizes the contributing area. Hydrological modelling and basin characterization both require this process. Catchment segmentation or dividing the catchment into separate land and channel segments, was used to examine the catchment's dynamics. This is utilized to characterize and investigate happenings in one region of the research area against another. According to the distribution of the stream network, the basin is divided into nine different sub-catchments (Figure 2). Each catchment has a reach and an outlet. All streams within a sub-catchment flow into the outlet. The catchment region is the area where a single channel drains all streams that emerge from the area. The largest sub-catchment in the study region is number 1, while number 5 has the smallest. Ideally, each sub-catchment outlet should have a gauging station to effectively monitor the river discharge and subsequent dam operations in the basin.

Stream Density (S.D.)

The S.D. refers to the length of a stream per unit area (Horton 1945). The fora, climatic conditions, relief, and infiltration rate all impact the stream density of any place (Nag 1998). The basin's S.D. varies from 0 to 0.4 km/km^2 (Figure 3a). Minimal S.D. indicates that surface runoff potential is low; however, infiltration capacity is also significant, depending on precipitation intensity. The presence of permeable rocks with low relief and a low S.D. implies thick vegetation (Biswas *et al.* 2014; Asfaw and Workineh 2019). High S.D. indicates a greater risk of surface runoff and erosion.

Floods are more likely to occur in areas with high drainage density values, so caution should be exercised in such regions. Necessary infrastructures should be put in place for a proper drainage system to avert flooding in such areas in the basin.

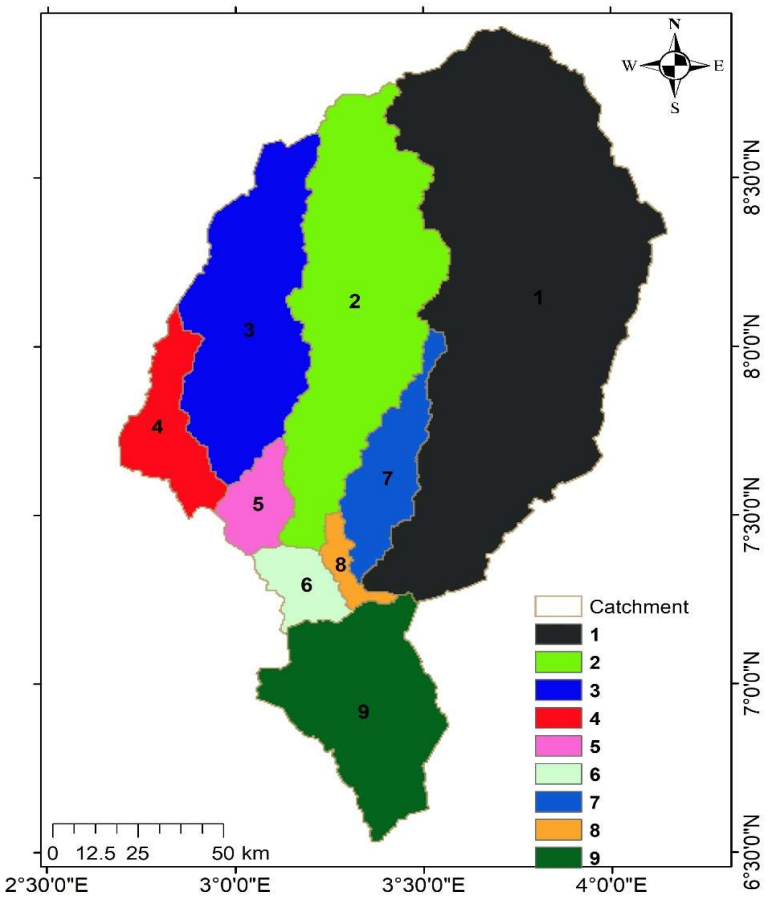

Figure 2: Catchment Delineation

Stream Frequency (S.F.)

For each unit area, this represents the number of stream segments (Horton 1945). As illustrated in Figure 3b, the Basin's S.F. range from 0.002 to 0.8 /km^2. Areas with low S.F. have reduced runoff due to low infiltration. Thus, flooding is less likely (Markose and Jayappa 2011, Carlston 1963). However, high S.F. areas are vulnerable to flood and erosion (Biswas et al. 2014).

Stream Order (S.O.)

Due to its simplicity, Strahler's (1964a, b) ordering method was utilized in this investigation (Adeyeri et al. 2017a; Asfaw and Workineh 2019; Arabameri et al. 2020). According to the findings, the basin contains 2148 streams connected by four-stream orders (Figure 3c, Table 1). The basin order is the highest stream order in a basin (Umrikar 2017). As a result, the ROSB is considered a fourth-order basin system. The first stream order has the longest stream length (> 200 km^2), followed by the second, third, and fourth in descending order (Figure 4). Higher stream order is connected to water, sediment, and nutrient ejection (Hajam et al. 2013). As a result, the ROSB has a dendritic drainage pattern.

Infiltration Number (I.N.)

It is determined by the density of the drainage system and the frequency of the streams. According to Prabhakaran and Raj (2018), the I.N. reflects a basin's water transmission potential. According to Faniran (1968), areas with lower I.N. indicate more substantial

infiltration and lower surface runoff; however, this is only true if the precipitation rate does not exceed the infiltration rate. On the other hand, considerable I.N. values indicate minimal water infiltration and high surface runoff. The majority of low I.N.s are found to the north of the basin, whereas most high I.N.s are located to the south (Figure 3d).

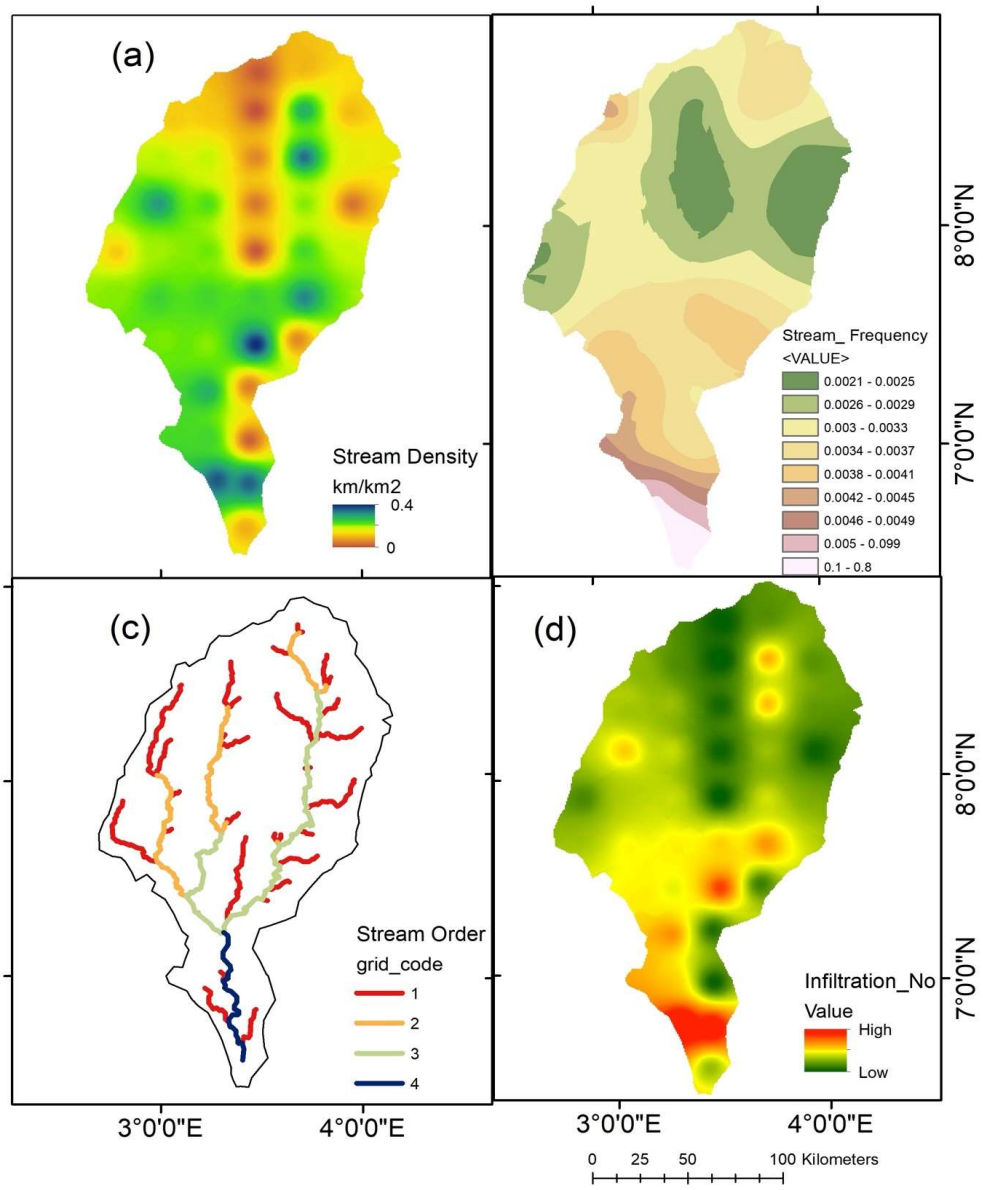

Figure 3: Distribution of (a) Stream Density (b) Stream Frequency (c) Stream Order, (d) Infiltration Number

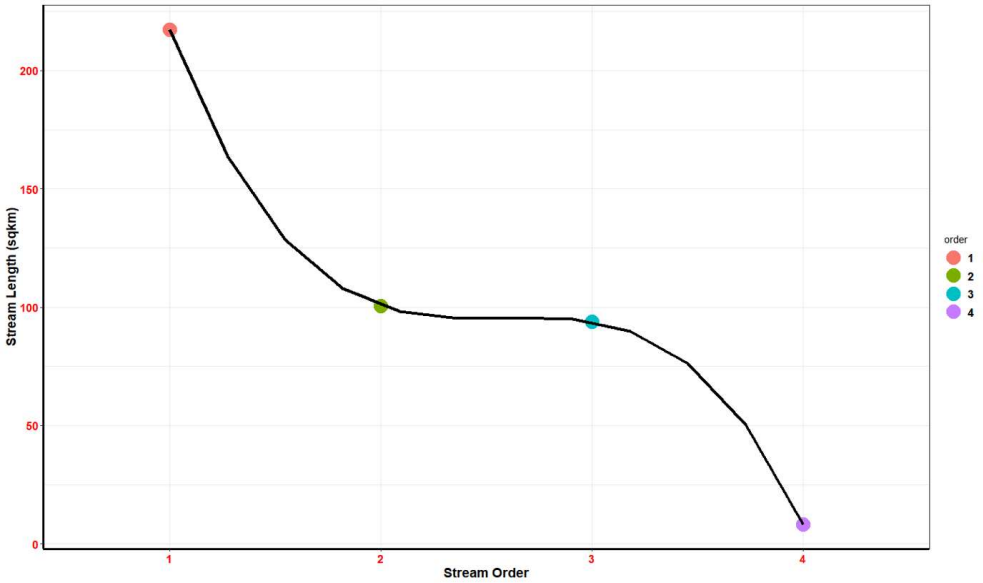

Figure 4: Stream Length vs Stream Order

Stream Number (S.N.)

A total of 2148 streams were retrieved, with 1017 being first-order streams, 441 being second-order streams, 517 being third-order streams, and 173 being fourth-order streams (Table 1). As the stream order grows, the number of streams usually reduces in geometric progression (Horton 1945).

The first and second stream orders, which account for 47.3 percent and 20.5 percent of the total, are seasonal and originate in mountains and hills with a steep/moderate slope. This supports Pophare and Balpande's (2014) findings that differences in the rock structure cause different stream orders. The basin's third stream order accounts for 24.1 percent of the basin's total area, exhibiting morphological changes. The 4th order accounts for 8.1 percent, mainly found in catchment planes with strong erosion features and loads of sediments.

Horton's laws of stream numbers emphasized that when the number of stream segments of each order is plotted against the order, the number of stream segments of each order forms an inverse geometric sequence. He opined that most stream networks show a linear relationship with only a minor deviation from a straight line. Regression analysis was also used to validate the data and produce more precise results in order to show potential links and measure their strength.

The best-fitted model for illustrating the relationship between stream order and stream number is indicated by R^2 values. For example, the R^2 values of 0.8 and 0.7 show that stream number and order are highly correlated (Figure 5).

Stream length (S.L.)

The basin has a total length of 420 km^2 of stream sections. The cumulative stream length of the first-order streams is approximately 217 kilometres, whereas the overall stream length of the fourth-order stream is 8.2 kilometres (Table 1). The overall length of stream segments is greater in first-order streams and diminishes as the stream order increases. This is due to high-altitude streams, relief variations, a moderately steep slope, and possible uplift in the basin (Horton 1945).

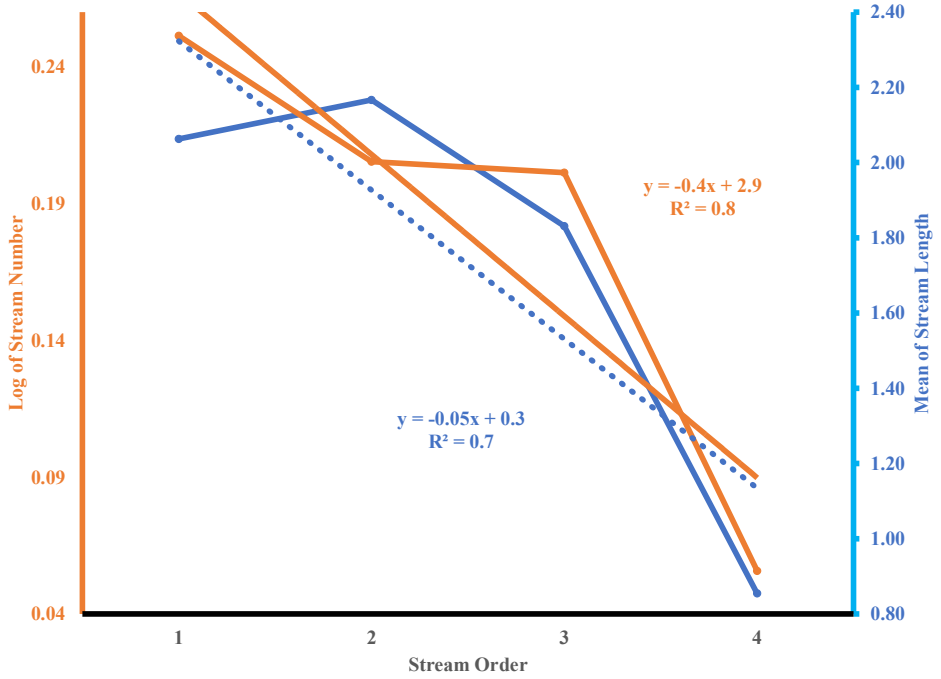

Figure 5: Log of stream number vs stream order, and the mean stream length vs stream order

Table 1: Morphometric Parameters

SO	SN	%	S.L. (km)
1	1017	47.3	217.3
2	441	20.5	100.5
3	517	24.1	94.0
4	173	8.1	8.2
TOTAL	2148	100	420.0
Bifurcation Ratio			
1st Order/ 2nd Order	2nd Order/ 3rd Order	3rd Order/ 4th Order	Mean
2.3	0.9	3.0	2.0

Drain Area and the Longest Flow Path

The catchment drains into a drainage line, which is known as the drain area. This is the sum of the catchment and adjacent catchment areas that are connected to the drainage line.

In fluvial geomorphology, drainage basins/drain areas are the most important hydrologic units to consider. A drainage basin is the source of water and silt that flows down the river system from higher elevations to lower elevations, reshaping the channel shapes. Drainage basins have a crucial role in ecology. Water can pick up nutrients, silt, and contaminants as it flows over land and along rivers. They are transported with the water to the basin's outlet, where they can alter ecological processes both along the way and in the receiving water source. The higher the drain area, the greater the volume of water linked with it. This means that streams with higher drain areas are more likely to overflow, affecting the physiology of the nearby environment. Figure 6 and Table 2 shows that sub-catchment 1 has the highest drain area of 9341.8 km^2. This also corresponds to the longest flow path, covering 266 m (Table 3). Sub-catchment 8 has the lowest drain area of 232 $km^{2,}$ while the flow path covers 41 m. Further statistics on the longest flow path is presented in Table 3.

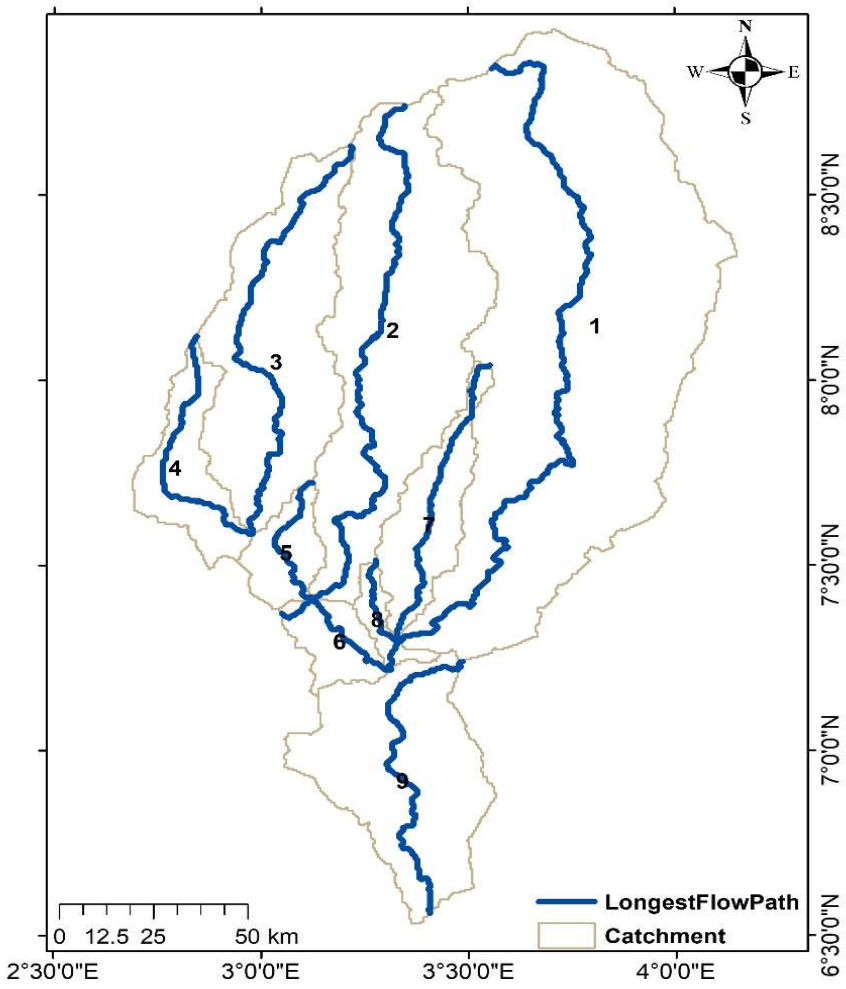

Figure 6: Longest flow path for each catchment

Table 2: Drain area and perimeter of the longest flow path

Path	Perimeter_	Drain Area_SQKM
1	694.8	9341.8
2	518.7	4285.3
3	387.8	2963.0
4	236.7	936.6
5	137.6	524.8
6	132.8	489.8
7	269.4	1011.8
8	129.9	231.5
9	314.7	2477.0

Table 3: Statistics of the longest flow path

Path	Length (m)	Slp (m/km)	Slp1085 (m/km)	Upstream Elevation (m)	Downstream Elevation (m)	Elev10 (m)	Elev85 (m)

1	266.0	45.2	35.1	483.0	52.0	80.0	331.0
2	200.8	47.9	39.2	416.0	71.0	96.0	308.0
3	155.0	49.6	38.4	392.0	116.0	137.0	297.0
4	84.9	59.4	37.2	298.0	117.0	136.0	221.0
5	48.7	98.4	74.8	237.0	65.0	72.0	170.0
6	47.1	93.4	36.3	202.0	44.0	47.0	93.0
7	100.2	91.5	74.2	382.0	53.0	72.0	272.0
8	40.6	101.6	102.5	192.0	44.0	44.0	156.0
9	112.7	49.7	30.7	201.0	0.0	3.0	96.0
Basin	372.3	36.2	30.7	483.0	0.0	12.0	320.0

ELEV 10: Elevation at 10% along the flow path from the outlet
Elev 85: Elevation at 85% along the flow path from the outlet
Slp1085: Slope along the line between the 10 percent point and 85 percent point
Slp: Slope along the line

Elevation Indicators

The regional distribution of several elevation indicators is depicted in Figure 7. VRM uses the change in three-dimensional orientation of grid cells within a neighbourhood to quantify terrain roughness. Terrain roughness is decoupled from slope or elevation by combining slope and aspect into a single measure. This is especially valuable for quantifying terrain characteristics for sediment movement, biological distribution, landform geomorphological evaluation, and landslide risk assessment (Sappington et al. 2007).

High roughness indicates stony soils with limited soil moisture, and low roughness indicates developed soils with higher moisture retention (Sappington et al. 2007). Low roughness is more pronounced in this basin. VRM can be used as proxy in soil moisture availability studies.

TRI shows the range of ruggedness in the basin is between 0 and 239, depicting level terrain surfaces to intermediately rugged surfaces. However, most of the distribution in the basin shows a level terrain surface. To determine geomorphological units, spatial variations in surface roughness are utilized to designate landform components and infer process information. At various scales, high terrain roughness is generally a signal of high species richness and biodiversity hot spots (Nichol et al. 2012). The roughness of the terrain also affects energy flows (current speed, wave energy and direction), sediment grain size, water column circulation, and nutrients dynamics, resulting in increased water column productivity. Furthermore, the aerodynamic flow, evaporation, hydrodynamic flows (including surface and ground water movement), runoff, and infiltration; and geomorphological processes like sediment transport and bank erosion are also influenced (Smith 2014).

TRASP has a significant effect on temperature. A slope slanted towards the sun and is not shadowed directly by the earth in the northern hemisphere. As a result, the southern side receives more solar radiation for a given surface area insolation.

Due to the prevailing winds, the north-facing slopes, for example, experience cooler temperatures; they are also shielded from direct sunshine during the dry season, resulting in more water available to nourish plants and forests. On the other hand, the south-facing slopes, which receive greater insolation, is hotter and dryer. In general, it determines the ecosystem of a basin based on its ability to absorb nutrients. For example, because the sun's rays are in the west at the hottest time of day in the afternoon, in most cases, a west-facing slope will be warmer than a sheltered east-facing slope (unless large-scale rainfall influences dictate otherwise). This can significantly affect altitudinal and polar limits of tree growth and the distribution of vegetation that requires large quantities of moisture. Thus, in most circumstances, a west-facing slope will be warmer than a sheltered east-facing slope since the sun's rays are in the west at the hottest time of day, in the afternoon (unless large-scale rainfall influences dictate otherwise). This could have a significant impact on tree growth's

altitudinal and polar limits, as well as the spread of moisture-loving plants.

In addition, increasing temperature increases the intensity of heavy precipitation by increasing air moisture (evapotranspiration), which accelerates the precipitation event through moisture convergence at low altitudes (Adeyeri et al. 2019). Due to the heavy precipitation intensity and consequent heavy river discharge, flooding events are expected in areas with south-facing slopes.

TWI is used to characterize biological processes such as forest site quality, vegetation patterns (Adeyeri et. al, 2017b) and yearly net primary output and quantify topographic influences on hydrological processes (Beven & Kirkby, 1979). The higher the TWI number, the wetter it is, and the lower the value, the dryer it is (Wilson and Gallant 2000).

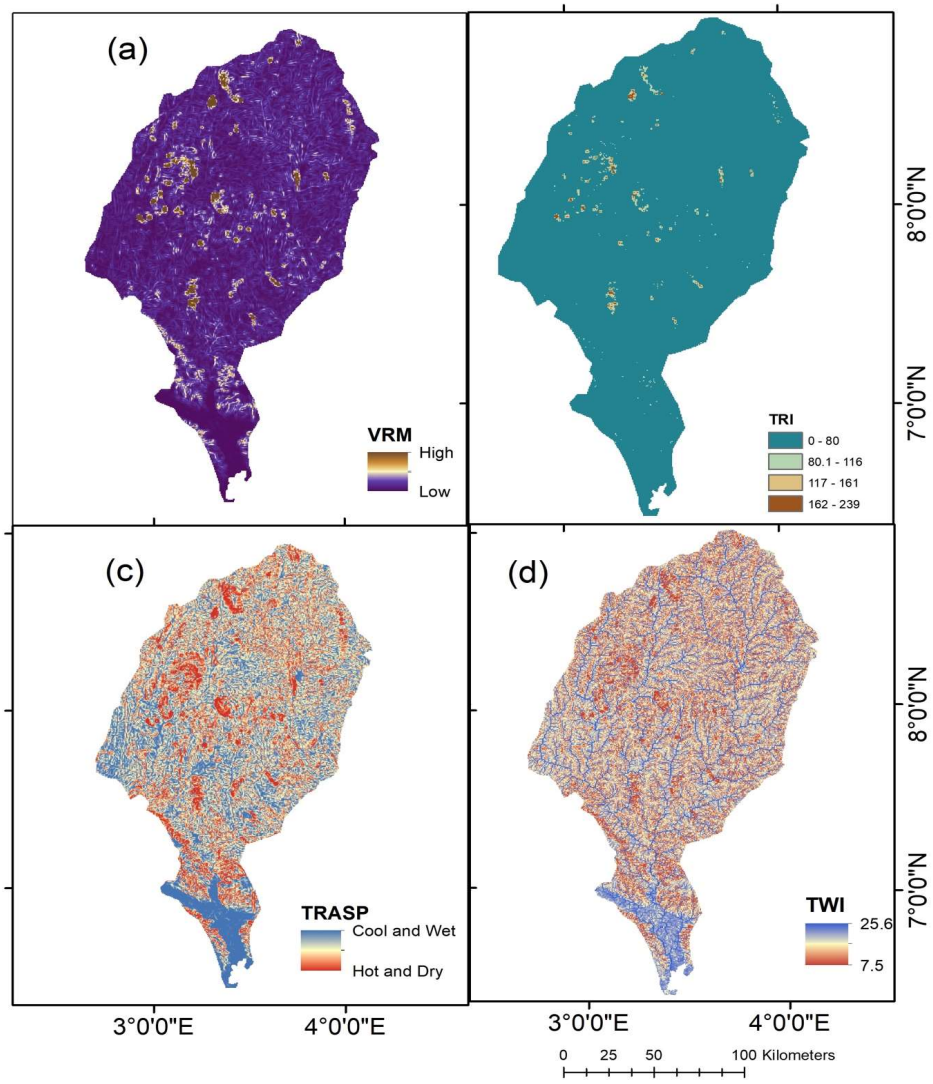

Figure 7: Spatial distributions of (a) VRM, (b) TRI, (c) TRASP and (d) TWI

The TWI value is high in lowland areas and along the primary channel, indicating a significant accumulation of water and high soil moisture, i.e., an excellent possibility for water harvesting. High TWI values can be used as a

proxy for detecting floodplains, wetlands, and diversity of fora and fauna species. The low TWI value is linked to steep slopes where water flows quickly, typical in the Basin's mountainous environment (Besnard et al. 2013).

Land use Dynamics

Changes in river discharges have been caused partly by human activities such as land-use land-cover (LULC) change, dam construction and operation, groundwater and surface water extraction, irrigation canals, and mining. Land usage has a significant impact on the fate of rain that falls on the ground. Most rain soaks into the soil (infiltrates) in a forest or grassy region, where it is subsequently absorbed by growing plants or percolates to groundwater. Over months, groundwater slowly seeps into streams, providing a consistent base flow (flow in streams when there is no rain) that fish and other aquatic species require. Most rain that falls on a parking lot, on the other hand, drains off quickly, often dripping. Besides this, the dynamics of the LULC over time could influence the biophysical compositions of the basin's thermal fields (e.g., Adeyeri and Okogbue, 2014; Ishola et al. 2016 a,b; Adeyeri et al. 2015; 2016; 2017 b, c; Ige et al. 2017; Abdullah et al. 2021). The size and location of the basin, elevation, land management and LULC types all influence how LULC changes affect river discharge.

The landuse transformation also determines the runoff regime (Adeyeri et al. 2019; 2020; Awotwi et al. 2017). However, before the landuse transformation, there is a need to understand the area coverage of each land use classes. In this basin, seven land use classes were observed: Forest, Settlement, Water Bodies, Cropland, Woodland Savanna, Bare Soil and Rock Outcrop for years 200 and 2019. Figures 8 and 9 present the spatial LULC classification for the two years, respectively. The area coverages are summarized in Table 4, while Table 5 shows the LULC transition from 2000 to 2019. In Table 4, the woodland savanna has the highest percentage of coverage in 2000 (41.1 %) while the water bodies have the least coverage of the total area (0.8%). However, in 2019, the highest percentage of coverage is cropland (30%). This is a rapid rise from 10% in 2000 to 30% in 2019.

Table 5 presents the dynamics of change between different LULC classes. For example, 149.2 and 219.1 km^2 of forest and cropland have been transformed to settlement between 2000 and 2019. In this case, the runoff peak is expected to increase (Li et al. 2001; Legesse et al. 2003; Adeyeri et al. 2020).

Table 4: LULC statistics

Year	2000	2019	2000	2019
LULC classes	**Area(sqkm)**	**Area (sqkm)**	**Area (%)**	**Area (%)**
Forest	5843.1	2955.6	25.6	13.0
Settlement	234.4	717.9	1.0	3.1
Water Bodies	175.9	161.5	0.8	0.7
Cropland	2417.6	6834.3	10.6	30.0
Woodland Savanna	9370.6	5609.4	41.1	24.6
Bare Soil	2430.4	5534.8	10.7	24.3
Rock Outcrop	2328.4	987.0	10.2	4.3
Total	22800.4	22800.4	100.0	100.0

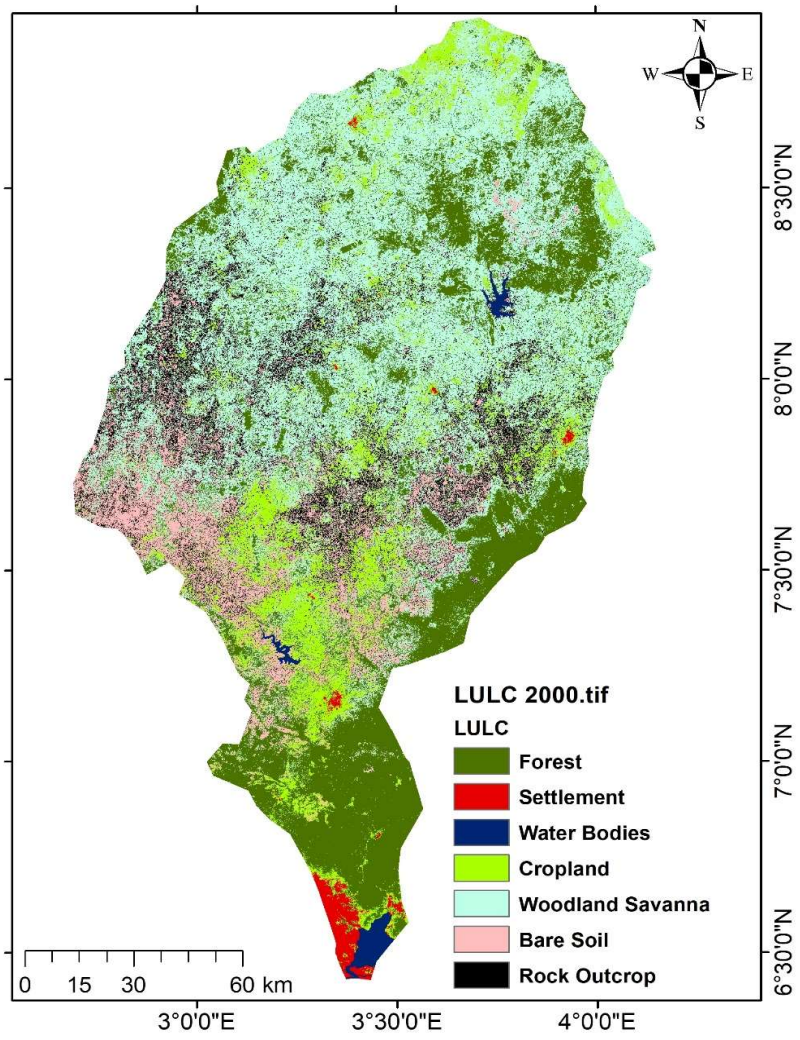

Figure 8: LULC classification for year 2000

Figure 10 further explains the relative change rate in the distribution of LULC (%/period). Positive means increase, negative means decrease. The relative change shows that rock outcrop and forest decreased by 135.9% and 97.7%, respectively. The dynamics of this change is seen in Table 5 as most rock outcrops that have been converted to bare soil (980.2 km^2) due to the quarry activities. However, most forests have been converted to cropland (1363.9 km^2).

The highest gain is seen in settlement (67.3 %). The dynamics (Table 5) shows that most croplands (219.1 km^2) have been converted to settlements. Although there is a gain in the cropland, these gains are primarily from woodland savannah (3122 km^2). Various transformations between LULC classes could affect and modify the basin's hydrology (Qiu et al. 2016; Adeyeri et al. 2020).

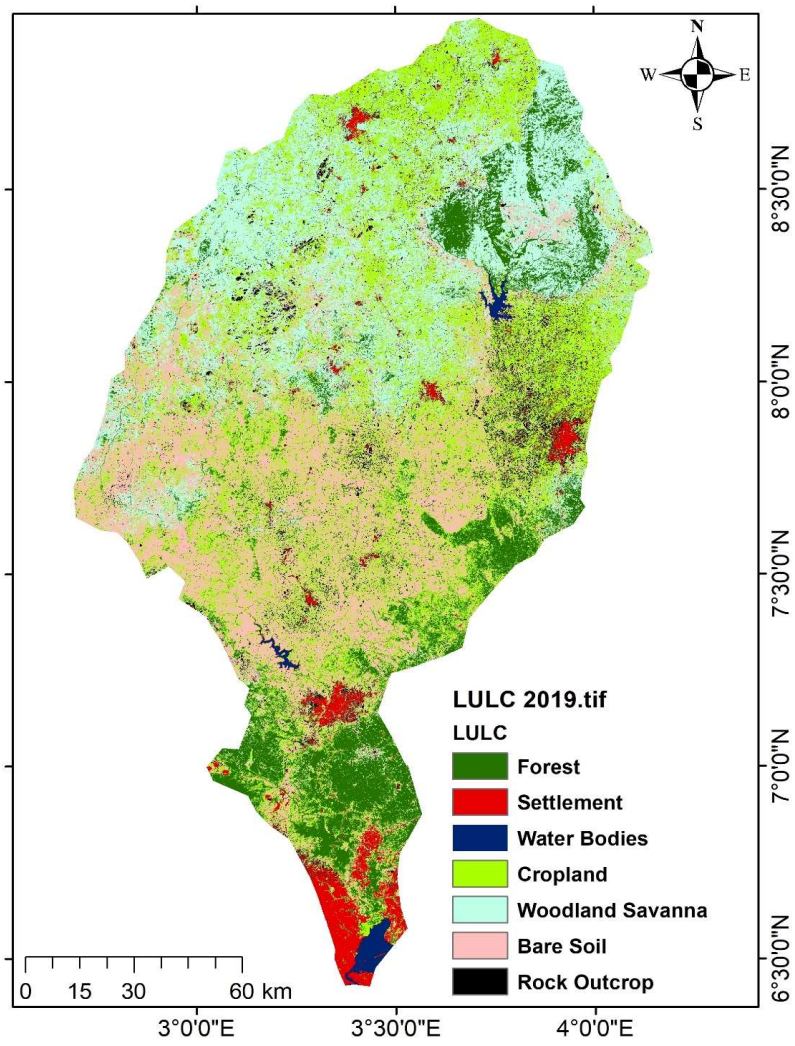

Figure 9: LULC classification for the year 2019

Table 5: LULC transition dynamics from 2000 to 2019 (Sqkm)

LULC	Forest	Settlement	Water Bodies	Crop land	Woodland Savanna	Bare Soil	Rock Outcrop
Forest	2282.0	149.2	0.4	1363.9	1311.6	648.7	85.3
Settlement	0.4	225.9	0.2	4.3	0.4	1.2	2.1
Water Bodies	0.1	12.8	159.1	1.6	0.0	0.4	1.8
Cropland	37.9	219.1	0.3	998.4	228.8	685.9	246.5
Woodland Savanna	507.4	75.8	0.0	3122.0	3389.1	1894.1	378.9
Bare Soil	92.2	10.1	1.2	674.2	240.5	1322.4	89.0
Rock Outcrop	34.6	24.8	0.2	667.6	437.1	980.2	183.1

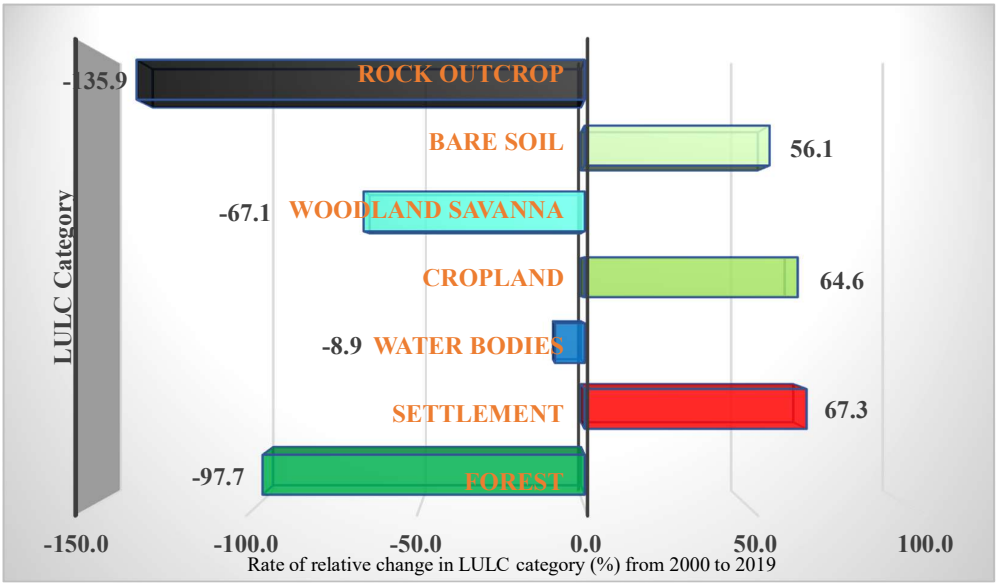

Figure 10: Rate of relative change in the distribution of LULC category (%) from 2000 to 2019

CONCLUSION

To statistically and qualitatively examine the morphometry and LULC dynamics in the ROSB, a combination of digital elevation model and LULC classification are used. The ROSB is drained by four-stream orders, with the first and second-order streams jointly accounting for 68 percent of the total stream order. As evident in the stream frequency, infiltration number, and drainage density analysis, the potential for surface runoff, flood, and erosion differ across the basin. The ROSB has a lot of potential, especially in agriculture, power generation, water management, and food security. Catchment parts with 4th order streams fit dam construction which could be subsequently used for irrigation farming, power generation and domestic water supply. In regions with 1st and 2nd stream order, a water harvesting structure may be required to monitor the speed of surface runoff. Although drainage density varies across the basin, catchments with high drainage density should be considered for year-round agricultural and power generation. Drainage infrastructure would be necessary to convey runoff to streams in areas with high drainage density. In the study area, seven LULC classes were observed: Forest, Settlement, Water Bodies, Cropland, Woodland Savanna, Bare Soil and Rock Outcrop for years 200 and 2019. 149.2 and 219.1 km^2 of forest and cropland has been transformed respectively to settlement between 2000 and 2019. In this case, the runoff peak is expected to increase. However, in this study, we could not directly compare the relationship between the morphometric parameters and the LULC dynamics because the digital elevation model used is static. Future studies should use more dynamical elevation models.

ACKNOWLEDGEMENTS

The research team appreciates the United States Geological Survey for providing the datasets used and the Tertiary Education Trust Fund (TETFund) for funding this study in the 2019 National Research Fund (NRF) Grant Cycle.

REFERENCES

Abdullah, A.F., Abdullah, A.K., Abdullah, A.R., Akter K., Jahir, D., Sikdar, S., Ashrafi T., Mallik, S. and Rahman, M. (2021). Assessing and predicting land use/land cover, land surface temperature and urban thermal field variance index using Landsat imagery for Dhaka Metropolitan area. Environmental Challenges. https://doi.org/10.1016/j.envc. 2021. 100192.

Adeyeri, O.E. and Okogbue, E.C. (2014). Effect of landuse landcover on land surface temperature in Abuja using remote sensing and GIS techniques. In Proceedings of climate change, and sustainable economic development (pp. 175–184). ISBN 978-978-521-43-6-9.

Adeyeri, O.E., Okogbue, E.C., Akinluyi, F.O., Ishola, K.A. (2017c). Spatio-temporal trend of vegetation cover over Abuja using landsat datasets. International *Journal of Agriculture and Environmental Research*, 03(03) [ISSN: 2455–6939].

Adeyeri, O.E., Okogbue, E.C., Ige, S.O. and Ishola, K.A. (2015). Estimating the land surface temperature over Abuja using different landsat sensors. In Proceedings of climate change, environmental challenges and sustainable development (pp. 305–310). ISBN 978-978-53811-9-1.

Adeyeri, O.E., Akinsanola, A.A. and Ishola, K.A. (2017b). Investigating surface urban heat island characteristics over Abuja, Nigeria: relationship between land surface temperature and multiple vegetation indices. *Remote Sensing Applications: Society and Environment* 7:57–68.

Adeyeri, O.E., Ishola, K.A. and Okogbue, E.C. (2017a). Climate Change and Coastal Floods: The Susceptibility of Coastal Areas of Nigeria. *Journal of Coastal Zone Management* 20:443. doi: 10.4172/2473-3350.1000443

Adeyeri, O.E., Laux, P., Lawin, A.E., Ige, S.O., Kunstmann, H. (2019). Analysis of Hydrometeorological Variables over the transboundary Komadugu-Yobe Basin, *West Africa. Journal of Water and Climate Change.* https://doi.org/10.2166/wcc.2019.283

Adeyeri, O.E., Okogbue, E.C. and Akinluyi, F.O. (2016). Mapping evapotranspiration for different landcover of the Lake Chad area of Nigeria. *Journal of Remote Sensing Technology.* doi:10.18005/JRST0401005.

Adeyeri, O.E., Laux, P., Lawin, A.E. and Arnault, J. (2020). Assessing the impact of human activities and rainfall variability on the river discharge of Komadugu-Yobe Basin, Lake Chad Area. *Environment Earth Science* 79, 143. https://doi.org/10.1007/s12665-020-8875-y

Ajibade, L.T., Ifabiyi, I.P., Iroye, K.A. and Ogunteru, S. (2010). Morphometric Analysis of Ogunpa and Ogbere Drainage Basins, Ibadan, Nigeria. *Ethiopian Journal of Environmental Studies and Management*, Vol 3(1).

Arabameri, A., Tiefenbacher, J.P., Blaschke, T., Pradhan, B. and Bui, D.T. (2020). Morphometric analysis for soil erosion susceptibility mapping using novel GIS-based ensemble model. *Remote Sensing 12(5):874.*https://doi.org/10.3390/rs12050874

Asfaw, D. and Workineh, G. (2019). Quantitative analysis of morphometry on Ribb and Gumara watersheds: Implications for soil and water conservation. *International Soil and Water Conservation Research* 7(2):150–157. https ://doi.org/10.1016/j.iswcr.2019.02.003

Awotwi, A, Anornu, G.K., Quaye-Ballard, J., Annor, T., Forkuo, E.K. (2017). Analysis of climate and human impacts on runoff in the Lower Pra River Basin of Ghana. Heliyon 3(12). https://doi.org/10.1016/j.heliyon.2017.e00477

Besnard, A.G., La Jeunesse, I., Pays, O., Secondi, J. (2013). Topographic wetness index predicts the occurrence of bird species in foodplains. Diversity and Distributions 19(8):955–963. https://doi.org/10.1111/ ddi.12047

Biswas, A., Das Majumdar, D., Banerjee, S. (2014). Morphometry governs the dynamics of a drainage basin: analysis and implications. *Geography Journal* 2014:1–14. https://doi.org/10.1155/2014/927176

Buma, W.G., Lee, S.I.L., Seo, J.Y. (2016). Hydrological evaluation of Lake Chad basin using space borne and hydrological model observations. Water (Switzerland). https://doi.org/10.3390/w8050205

Bunmi, M.R., Yusuf, O.M., Oladapo, A.I. (2017). Morphometric Analysis of Asa and Oyun River Basins, North Central Nigeria. Geographical Information System. 5(6), 379–393. https://doi.org/https://doi.org/10.11648/j.ajce.20170506.20

Bolaji, G. A. and Bhattacharya, A. K. (2010). Fluid Flow Interactions in Ogun River. *International Journal of Research and Reviews in Applied Sciences*. 2(2).

Carlston, C.W. (1963). Drainage density and streamfow. *U.S. Geological Survey. Professional Paper*. No. 42, 2–C, 8pp.

Destouni, G., Jaramillo, F., Prieto, C. (2013). Hydroclimatic shifts driven by human water use for food and energy production. *Nature Climate Change* 3:213–217. https://doi.org/10.1038/nclimate1719

Ezeh, C.U., Mozie, A.T. (2019). Correction to: Morphometric analysis of the Idemili Basin using geospatial techniques. *Arabian Journal of Geosciences* 12(9):298. https://doi.org/10.1007/s12517-019-4469-y

Faniran, A. (1968). The index of drainage intensity—a provisional new drainage factor. *Australian Journal of Science* 31:328–330

Florinsky, I.V. (2017). An illustrated introduction to general geomorphometry. *Progress in Physical Geography*, 41: 723–752.

Forest Management Bureau (2011). Watershed characterization and vulnerability assessment using geographic information system and remote sensing. https://doi.org/https://doi.org/10.1109/isqed .2008.4479675

Hajam, R.A., Hamid, A., Bhat, S. (2013). Application of morphometric analysis for geo-hydrological studies using geo-spatial technology–A Case Study of Vishav Drainage Basin. *Hydrology Current Research*. https://doi.org/10.4172/2157-587.1000157

Hao, F.H., Chen, L.Q., Liu, C.M., Dai, D. (2004). Impact of land use change on runoff and sediment yield. J *Soil Water Conservation* 18(3):5–8

Horton, R.E. (1945). Erosional Development of Streams and their Drainage Basins; Hydrophysical Approach to Quantitative Morphology. *Bulletin of the Geological Society of America* 56, 2 75-370. https://doi.org/10.1177/030913339501900406

Ige, S.O., Ajayi, V.O., Adeyeri, O.E., Oyekan, K.S.A. (2017). Assessing remotely sensed temperature humidity index as human comfort indicator relative to landuse landcover change in Abuja, Nigeria. *Spatial Information Research.* 25, 523–533. https://doi.org/10.1007/s41324-017-0118-2

Ishola, K.A., Okogbue, E.C., Adeyeri, O.E. (2016b). A quantitative assessment of surface urban heat islands using satellite multitemporal data over Abeokuta, Nigeria. *International Journal of Atmospheric Sciences,* doi: http://dx.doi.org/10.1155/2016/3170789

Ishola, K.A., Okogbue, E.C., Adeyeri, O.E. (2016a). Dynamics of surface urban biophysical compositions and its impact on land surface thermal field. Model. *Earth Syst. Environ.* 2, 1–20. https://doi.org/10.1007/s40808-016-0265-9

Jia, Y.W., Zhao, H.L., Niu, C.W., Jiang, Y.Z., Gan, H., Xing, Z., Zhao, X. and Zhao, Z. (2009). A WebGIS-based system for rainfall-runoff prediction and real-time water resources assessment for Beijing. Computers and Geosciences 35(7):1517–1528

Legesse, D., Vallet-Coulomb, C. and Gasse, F. (2003). Hydrological response of a catchment to climate and land use changes in Tropical Africa: case study South Central Ethiopia. *Journal of Hydrology* 275(1):67–85

Li, W.H., He, Y.T., Yang, L.T. (2001). A summary and perspective of forest vegetation impacts on water yield. *Journal of Natural Resources* 16(5):398–406

Luo, Y., Su, B., Yuan, J., Li, H., Zhang, Q. (2011). GIS techniques for watershed delineation of SWAT model in plain polders. *Proceedings of Environmental Science* 10:2050–2057. https://doi.org/10.1016/j.proenv.2011.09.321

Markose, V.J., Jayappa, K.S. (2011). Hypsometric analysis of Kali River Basin, Karnataka, India, using geographic information system. *Geocarto International* 26(7):553–568. https://doi.org/10.1080/10106049.2011.608438

Mayomi, I., Yelwa, M.H., Abdussalam, B. (2019). Geospatial Analysis of Morphometric Characteristics of River Hawul Basin, North-East Nigeria. R*esources and Environment* 8(3):1–17. https://doi.org/10.5923/j.re.20180803.03

McCune, B. (2007). Improved estimates of incident radiation and heat load using non-parametric regression against topographic variables. *Journal of Vegetation Science* 18:751-754.

McCune, B., Keon, D. (2002). Equations for potential annual direct incident radiation and heat load index. *Journal of Vegetation Science*. 13:603-606.

Mohamad, I., Markus, M. (2009). Impacts of urbanization and climate variability on floods in northeastern Illinois. *Journal of Hydrologic Engineering* 14(6):606–616.

Nag, S.K. (1998). Morphometric analysis using remote sensing techniques in the Chaka sub-basin, Purulia district, West Bengal. *Journal of the Indian Society of Remote Sensing* 26(1–2):69–76. https://doi.org/10.1007/ BF03007341

Nichol, S.L, Anderson, T.J., Battershill, C., Brooke, B.P. (2012). Submerged Reefs and Aeolian Dunes as Inherited Habitats, Point Cloates, Carnarvon Shelf, Western Australia, in Seafloor Geomorphology as Benthic Habitat. In Book Elsevier, pp. 397-407. https://linkinghub.elsevier.com/ retrieve/ pii/B978012385140600027X

Odiji, C.A., Aderoju, O.M., Eta, J.B., Shehu, I., Adama, M., Onuoha, H. (2021). Morphometric analysis and prioritization of upper Benue River watershed, Northern Nigeria. *Applied Water Science* 11, 41. https://doi.org/10.1007/s13201-021-01364-x

Patel, D.P., Gajjar, C.A., Srivastava, P.K. (2013). Prioritization of Malesari mini-watersheds through morphometric analysis: a remote sensing and GIS perspective. *Environmental Earth Sciences*, 69(8), 2643-2656.

Pophare, A.M., Balpande, U.S. (2014). Morphometric analysis of Suketi river basin, Himachal Himalaya. India *Journal of Earth System Science* 123(7):1501–1515. https://doi.org/ 10.1007/s12040-014-0487-z

Prabhakaran, A., Jawahar, R.N. (2018) Drainage morphometric analysis for assessing form and processes of the watersheds of Pachamalai hills and its adjoining, Central Tamil Nadu, India. *Applied Water Science* 8(1):1–19. https://doi.org/ 10.1007/s13201-018-0646-5

Qiu, L., Peng, D., Xu, Z., Liu, W. (2016). Identification of the impacts of climate changes and human activities on runoff in the upper and middle reaches of the Heihe River basin, China. *Journal of Water and Climate Change* 7(1):251–262

Rastogi, R.A., Sharma, T.C. (1976). Quantitative analysis of drainage basin characteristics. *Journal of Soil and Water Conservation in India*, v.26 (1&4), pp.18-25.

Roberts, D.W., Cooper, S.V. (1989). Concepts and techniques of vegetation mapping. In Land Classifications Based on Vegetation: Applications for Resource Management.

USDA Forest Service GTR INT-257, Ogden, UT, pp 90-96

Sappington, J.M., Longshore, K.M., Thomson, D.B. (2007). Quantifying Landscape Ruggedness for Animal Habitat Analysis: A Case Study Using Bighorn Sheep in the Mojave Desert. *Journal of Wildlife Management*. 71(5):1419-1426

Singh, S., Kumar, S., Mittal, P., Kanhaiya, S., Prakash, P., Kumar, R. (2018). Drainage basin parameters of Bagh River, a sub-basin of Narmada River, Central India: Analysis and implications. *Journal of Applied Geochemistry*, 20(1), 91-102.

Smith, M.W. (2014). Roughness in the Earth Sciences. *Earth-Science Reviews*. Vol. 136, pp. 202-225. Available at: https://linkinghub.elsevier.com/retrieve/pii/S0012825214001081

Strahler, A.N. (1957). Quantitative analysis of watershed geomorphology. Eos Trans American Geophysical Union, https://doi.org/10.1029/TR038i006p00913

Strahler, A.N. (1964a). Quantitative geomorphology of basin and channel networks: *Handbook of Applied Hydrology*. Mcgraw Hill Book Company, New York

Strahler, A.N. (1964b) Part II. Quantitative geomorphology of drainage basins and channel networks. *Handbook of Applied Hydrology*. McGraw-Hill, New York, pp 4–39

Taofik, O.K., Innocent, B., Christopher, N., Jidauna, G.G., James, A.S. (2017). A comparative analysis of drainage morphometry on hydrologic characteristics of kereke and ukoghor basins on food vulnerability in makurdi town, Nigeria. *Hydrology*, 5(3): 32 https://doi.org/10.11648/j.hyd.20170503.11

Umrikar, B.N. (2017). Morphometric analysis of Andhale watershed, TalukaMulshi, District Pune, India. *Applied Water Science* 7(5):2231– 2243. https://doi.org/10.1007/s13201-016-0390-7